Plant Physiol. (1993) 101: 391–398

A Kinetic and Microautoradiographic Analysis of [^{14}C]Sucrose Import by Developing Wheat Grains[1]

Donald B. Fisher* and Ning Wang

Department of Botany, Washington State University, Pullman, Washington 99164

Assimilates enter developing wheat grains via a strand of phloem extending along the crease region of the grain. After phloem unloading, they move several hundred micrometers before being released into the endosperm cavity, from which they are absorbed by the developing endosperm. Extraphloem assimilate pools in the maternal tissue of the crease, therefore, play a central role in post-phloem transport. We investigated the location and turnover of ^{14}C-assimilates in the crease tissues and endosperm cavity sap by pulse labeling the flag leaf with $^{14}CO_2$. Sucrose accounted for >90% of ^{14}C at all times. Kinetic analysis of the crease sucrose pool and its depletion in excised grains showed that virtually the entire sucrose content of the crease tissues was involved in post-phloem transport and behaved basically as a single well-mixed compartment. Microautoradiographs also showed rapid movement of ^{14}C throughout most of the crease tissues. Quantification of ^{14}C concentration in the tissues showed a relatively shallow gradient of ^{14}C and, presumably, of sucrose through the nucellus and chalaza. The steepest gradient in ^{14}C content occurred in the vascular parenchyma between the chalaza and conducting cells (xylem and phloem).

Developing seeds provide particularly useful experimental systems for the study of phloem unloading and post-phloem transport. This is largely because they allow the interception of translocated solutes as they are released from maternal tissues into the apoplastic space around the developing embryo. Post-phloem transport in seeds, however, is a multistep process involving symplastic movement through a multicellular pathway composed of several distinct tissues, plus transmembrane movement into the apoplast (O'Parka, 1990). Confident interpretation of experimental results depends on an adequate understanding of the pathway of assimilate movement and compartmentation within the maternal tissues of the seed. This is especially true of experimental treatments that alter the rate of assimilate release into the apoplast (Gifford and Thorne, 1986; Ellis and Spanswick, 1987; Minchin and Thorpe, 1989).

We have recently developed a method for perfusing the endosperm cavity of intact, attached wheat grains to study these transport steps. (A preliminary report appears in Patrick et al., 1991.) Wheat grains offer distinct advantages for this work because, in addition to the ability to measure solute concentrations in the apoplast between the maternal and embryonic tissues (i.e. in the endosperm cavity), similar measurements can be made for the grain sieve tubes (Fisher and Gifford, 1986). Also, the presence of an apoplastic barrier between the grain phloem and endosperm cavity (Zee and O'Brien, 1970) greatly simplifies questions concerning apoplastic solute movement of both assimilates and applied solutions.

The present experiments were undertaken to characterize the dynamics of sucrose pools and their location in the maternal tissues of the wheat grain through which assimilates pass on their way to the endosperm. Some observations are available on this topic (Jenner, 1974; Sakri and Shannon, 1975; Donovan et al., 1983; Ho and Gifford, 1984; Lingle and Chevalier, 1984; Ugalde and Jenner, 1990), but they are not sufficiently detailed for quantitative compartmental analysis. Our aim was to develop a compartmental model of sucrose pools within the maternal grain tissues by following ^{14}C kinetics at several points along the transport pathway from the peduncle phloem to the endosperm cavity and to localize the sites of these pools within the tissues.

MATERIALS AND METHODS

Plant Material

Plants of *Triticum aestivum* L. (cv SUN 9E) were grown in a growth chamber on a 16-h photoperiod at a light intensity of 450 μE m^{-2} s^{-1}. The temperature was 22°C during the day and 16°C at night. The plants were grown in pots containing equal volumes of perlite, vermiculite, and potting soil and were irrigated with water at 16-h intervals, and a complete nutrient solution was supplied once a week. Experiments were run with plants in the linear phase of grain filling, 15 to 25 d after anthesis. Grain filling was complete at about 30 d postanthesis.

$^{14}CO_2$ Labeling and Sample Collection

Experiments were run at ambient laboratory temperature (about 22°C) under a water-filtered metal halide lamp providing illumination of about 800 μE m^{-2} s^{-1}. The distal one-third of the flag leaf blade was allowed to assimilate 250 μCi of $^{14}CO_2$ for 10 min in a sealed chamber, and, 1 h later, the labeled portion of the flag leaf was cut off. This generated a sharp pulse of labeled translocate without affecting sieve tube solute concentration or the grain-filling rate (Fisher, 1990).

The transport pathway was sampled at four points: the peduncle sieve tubes, grain pedicel sieve tubes, crease tissues, and the endosperm cavity. Peduncle sieve tube exudate was

[1] This work was supported by grants from the U.S. Department of Agriculture (88-37262-3426) and the National Science Foundation (DCB-9019411).

* Corresponding author; fax 1-509-335-3517.

obtained from about 20 exuding aphid stylets (Fisher and Frame, 1984). At each sampling time, accumulated exudate was dissolved in several microliters of water, transferred to a preweighed square of aluminum foil, dried in a vacuum dessicator, and weighed on a Cahn electrobalance. Phloem exudate was collected from the broken pedicel of each grain removed for sampling (Fisher and Gifford, 1986), and the exudate was dissolved in 200 μL of water. Two grains were removed at each sampling time. Endosperm cavity sap was obtained by slicing off the distal one-fourth of the grain and sucking out the sap with a fine-tipped pipet. Crease tissues, consisting essentially of a small amount of pericarp plus the vascular tissues, chalaza, and nucellus (Fig. 1), were placed in a test tube containing 1 mL of water in a boiling water bath for 2 min to inactivate invertase.

Assays and Metabolite Fractionation

Aliquots of appropriate volumes were assayed enzymically for sucrose, glucose, and fructose by the direct fluorometric procedure of Jones et al. (1977). The remaining sample was separated into acidic, basic, and neutral fractions by passage through Sephadex ion exchange columns (Redgwell, 1980). ^{14}C-Metabolites in each fraction were separated by two-dimensional cellulose TLC (von Arx and Neher, 1963) and autoradiographed with x-ray film.

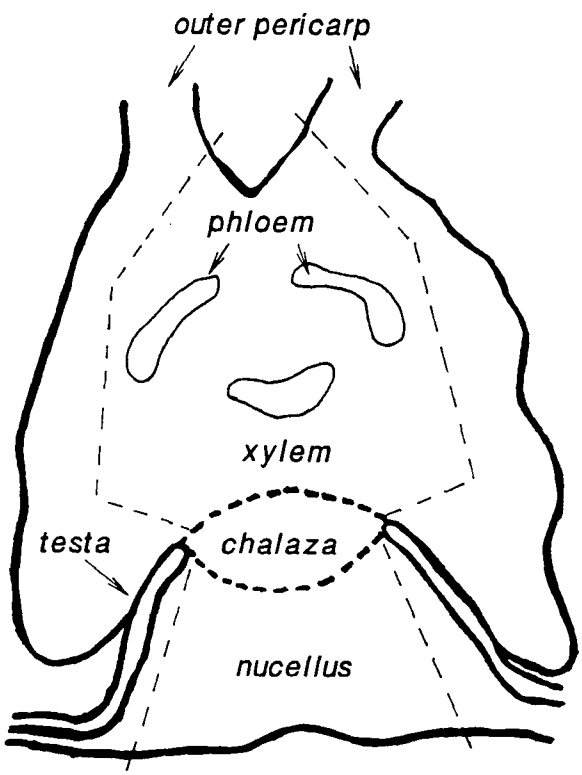

Figure 1. Diagram of tissues in a cross-section of the crease region of a wheat grain. The diagram should be compared with the autoradiographs in Figure 4. Crease samples also included small and variable amounts of inner pericarp, as well. Specific activities on a unit volume (section weight) basis were determined for tissues within the dashed lines (Fig. 6).

Microautoradiography and Specific Activity Measurements of Sectioned Crease Tissues

The labeling protocol for microautoradiography was similar to that described above, except 1.0 mCi of $^{14}CO_2$ was used for labeling. Peduncle stylet exudate was collected, and its specific activity was measured (dry weight basis) to determine the times at which grains were to be frozen for microautoradiography. A single grain was removed at each sampling time, and the crease tissues from the middle one-half of the grain were rapidly dissected out and plunged into isopentane:methylcyclohexane (9:1, v/v) cooled with liquid nitrogen. The frozen length of crease tissues was covered with dry ice and several segments 1 mm or less in length were cut from the central half. These pieces were freeze substituted in acetone, embedded in epoxy resin, sectioned, and stained with the periodic acid-Schiff reaction before coating with Ilford L4 nuclear emulsion (Fisher and Housley, 1972).

Distribution of ^{14}C in the epoxy-embedded crease tissues was quantified by weighing and counting of microtome sections. Starting at the nucellar surface, longitudinal sections were cut with glass knives, without water, at nominal thicknesses ranging from 4 to 6 μm. Desired tissue areas were cut from each section under a dissecting microscope with a razor blade fragment (Fig. 1). Samples from three to five successive sections were pooled and weighed on a Cahn electrobalance capable of weighing to ±0.1 μg (sample weights ranged from 2–6 μg). After the sections were weighed, they were floated on a drop of water on an adhesive-coated microscope slide, stretched by heating, and dried without removing the water. After the sections were counted with a thin end-window Geiger-Muller tube, they were stained with toluidine blue, mounted in epoxy resin, and examined microscopically to identify the tissues included in each sample. The distance of each sample from the nucellar surface was estimated from a combination of section thickness, number of sections per sample, and presence of position landmarks (e.g. chalaza, xylem vessels) visible in the autoradiographs of cross-sections taken from the same crease specimen.

Silver grain densities were also determined by video densitometry (data not shown). The results were somewhat difficult to present visually and did not result in an impression much different from the microautoradiographs themselves. However, comparison of the two approaches to quantifying ^{14}C distribution revealed probable discrepancies, especially in the nucellus (lower silver grain densities than expected on the basis of activity per unit section volume). For clarification, serial longitudinal sections were taken from another block, and the proportion of soluble and retained ^{14}C was determined for each sample of sections, taking care not to lose sections or section fragments. Total ^{14}C for each sample was determined as above, and the sections were recounted after washing away soluble ^{14}C with water. (It was not possible to recount section samples from the earlier blocks because some of the weighed sections and fragments had been lost during the staining process.)

Compartmental Modeling

The kinetics of [^{14}C]sucrose labeling in the wheat grain were modeled by standard compartmental analysis (Shep-

pard, 1962). The resulting set of simultaneous first-order differential equations were solved numerically on a microcomputer using a commercial software program (TUTSIM Products). With an important correction (see "Results"), the measured kinetics of [^{14}C]sucrose-specific activity in the sieve tubes were used as input kinetics for the model. Pool sizes and transport rates were taken from the sucrose assays and from transport rates previously measured for plants growing under the same conditions (Fisher, 1990).

RESULTS

Form of ^{14}C

The neutral fraction, all [^{14}C]sucrose, accounted for >90% of the ^{14}C in almost all samples (Table I). For this reason, only overall averages are presented for the ion exchange fractionations. However, there was a discernible increase in the proportion of ^{14}C in the amino acid and organic fractions in the crease tissues and endosperm cavity sap. In each, the amino acid ^{14}C increased from about 3 to 7% of the total radioactivity from the earliest to the latest sample, and organic acids increased from about 1 to 3%.

Eight to 12 labeled amino acids were detected in most samples, with Glu, Ala, and Ser, in that order, labeled more strongly than others. This reflected their relative proportions on plates sprayed with ninhydrin, as well as amino acid analyses from similar plants (Fisher and Macnicol, 1986). In crease extracts, Asp and especially Glu were also labeled prominently. About six compounds were labeled in the organic acid fractions, but none could be identified confidently.

Because nonsucrose compounds represented such a small proportion of ^{14}C at all times, no further attempt was made to quantify their separate contribution to the overall labeling kinetics. Calculations of sucrose-specific activities assumed that all of the activity was in the form of sucrose.

Kinetics of [^{14}C]Sucrose along the Transport Pathway

Four experiments were run in which the kinetics of [^{14}C]-sucrose were followed in the peduncle sieve tubes, grain pedicel sieve tubes, crease tissues, and endosperm cavity. Results of one experiment are shown in Figure 2. Major features of the other experiments were similar, but, for all, there was more variability in the data for crease and cavity sap specific activities than for the phloem exudates. Data are not presented for exudate specific activities on a dry weight basis, because sucrose accounted for a fairly constant proportion (about 75%) of exudate dry weight.

Table I. *Distribution of ^{14}C among sugars, amino acids, and organic acids*

Fractionation by ion exchange columns. Because there was only a slight trend with time (see text), the values presented are averaged over all times ± SE.

	Sugars	Amino Acids	Organic Acids
		% total ^{14}C	
Stylet exudate	97.7 ± 0.8	1.8 ± 0.7	0.50 ± 0.17
Crease tissues	93.0 ± 2.3	4.9 ± 1.6	2.2 ± 0.7
Endosperm cavity	92.2 ± 2.9	5.7 ± 1.7	2.0 ± 0.9

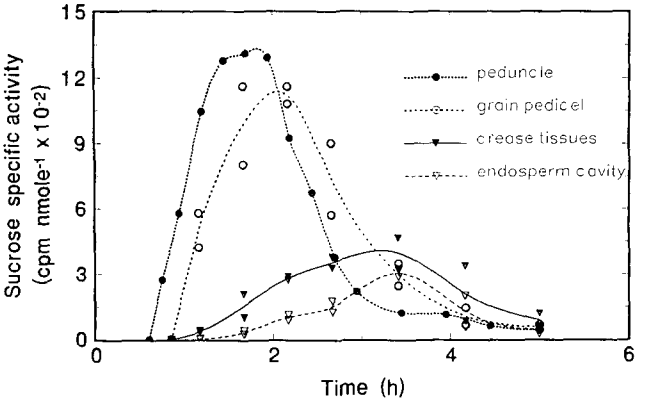

Figure 2. [^{14}C]Sucrose kinetics at four points along the translocation pathway into the wheat grain.

For purposes of later comparisons with possible compartmental models, several features of the kinetics are of importance. First, the maximum specific activity in the crease and endosperm cavity reached similar values but only at 25 to 30% of that in the sieve tubes. Second, there was a substantial delay in the increase of sucrose specific activity in the endosperm cavity, presumably reflecting a "pooling delay" in movement of ^{14}C through the crease tissue sucrose pool after phloem unloading. Finally, although not reflected in the experiment illustrated in Figure 2, in two experiments the decline in specific activity in the crease and cavity was slower, decreasing by one-half in approximately 2 h after reaching a maximum.

Microautoradiography

The kinetics of stylet exudate specific activity in the plant used for microautoradiography are shown in Figure 3, which also indicates the times at which crease samples were frozen.

Microautoradiographs of the crease tissues are shown in Figure 4, A to C. For comparison, an unexposed section (Fig.

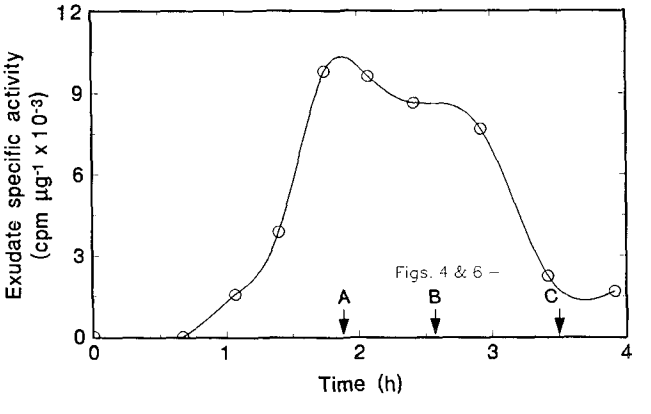

Figure 3. Kinetics of phloem exudate ^{14}C collected from exuding stylets on the peduncle during an experiment in which crease tissues were frozen for microautoradiography (arrows).

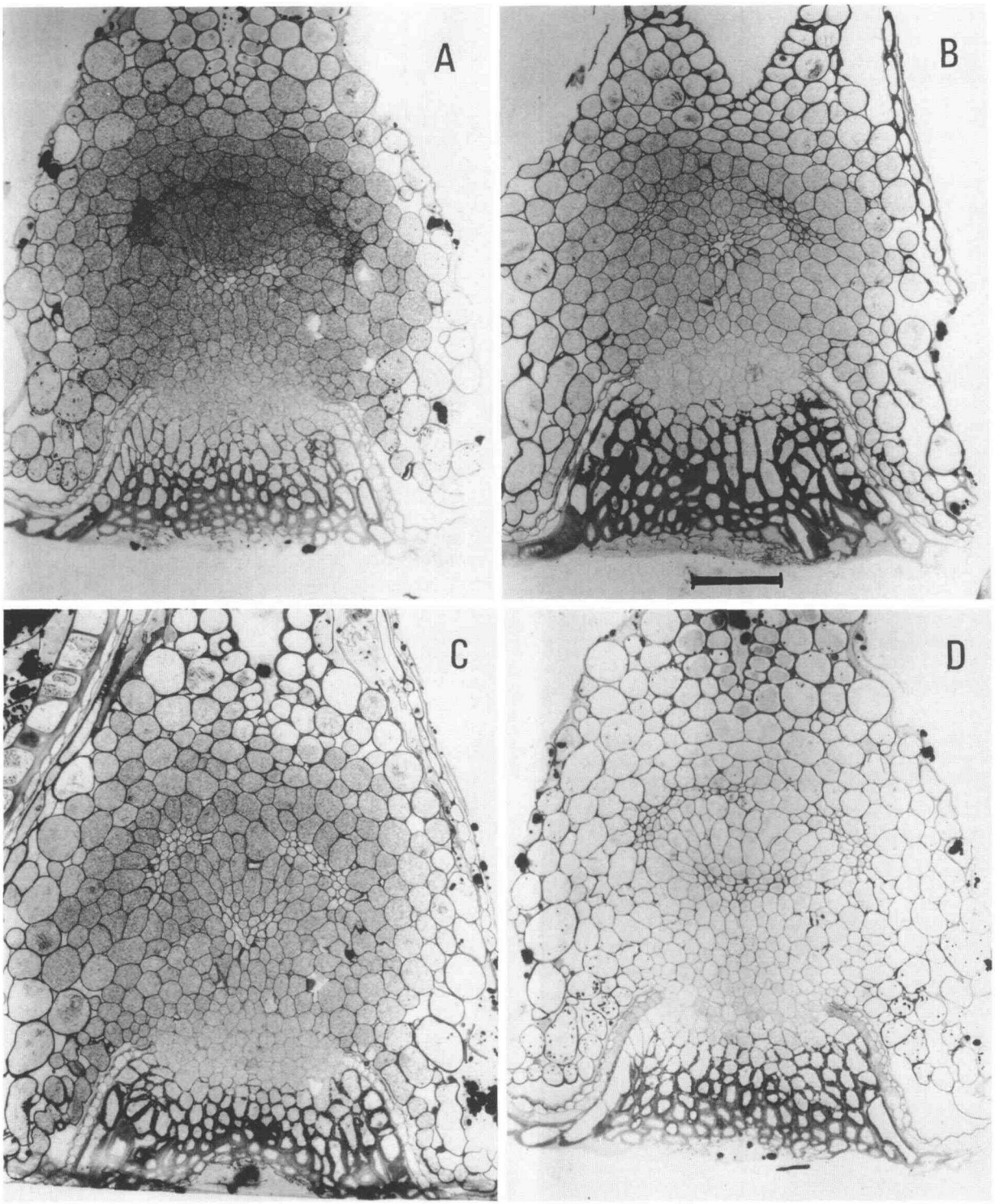

Figure 4. Microautoradiographs of [^{14}C]sucrose distribution in crease tissues sampled at the times indicated in Figure 3. *D* is not an autoradiograph and, for comparison, shows the pattern of periodic acid-Schiff staining alone. Bar = 100 μm.

4D) shows the pattern of staining by the periodic acid-Schiff reaction alone. Individual silver grains are not visible at this relatively low magnification, which was chosen to illustrate the overall pattern of ^{14}C distribution. Instead, variations in grain density are evident as shades of gray over the cell lumina.

Aside from the phloem, where the striking differences in grain densities clearly reflect the sampling times, the autoradiographs are probably most notable for their similarities. Unloaded [^{14}C]sucrose appeared to be distributed rapidly throughout the vascular parenchyma, with substantially less movement to the crease periphery. In contrast to the completely unpigmented vascular parenchyma cells, these outer cell layers of the crease consist of green pericarp cells. In the micrographs of Figure 4, the pericarp may be distinguished by the presence of intercellular spaces.

Although the crease cells are vacuolate to varying degrees depending on the tissue, there was no evidence of vacuolar/cytoplasmic compartmentation, comparable to observations of companion cells (Christy and Fisher, 1978; Fisher, 1978). Labeling over the nucellus and chalaza was markedly lower than over the vascular parenchyma. Somewhat surprisingly, in view of justifiable speculation that the chalaza might represent a significant resistance to assimilate movement (Zee and O'Brien, 1970), the sharpest gradient in grain density was not within the chalaza or across its border but in the vascular parenchyma cells between the chalaza and the xylem and phloem. This appearance was confirmed by the data for grain densities (data not shown).

However, the autoradiographic observations were distorted, at least over the nucellus, by a substantially lower retention of label in that tissue on exposure of the sections to water (Fig. 5). For most of the crease tissues, retention of ^{14}C in the sections was quite high (about 60%) and uniform. Starting at the chalaza, retention decreased sharply toward the nucellar surface, declining as low as 14%. This decrease was associated with an increase in the wall thickness of nucellar cells. However, there was no indication of a difference in grain densities over the walls versus the cell lumen. The reason for retention of soluble ^{14}C in epoxy sections on exposure to water is unclear in any event (Fisher and Housley, 1972).

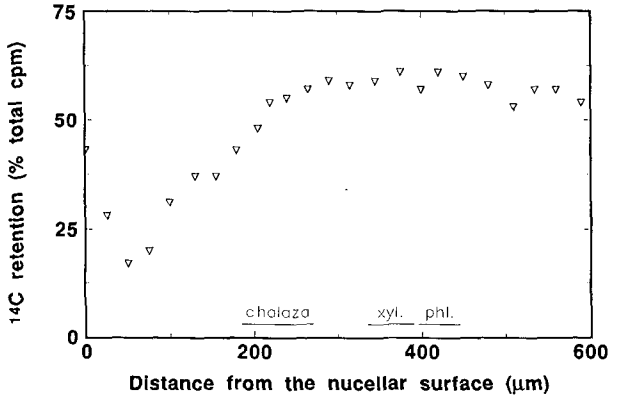

Figure 5. Retention of ^{14}C on exposure to water of longitudinal sections from epoxy-embedded crease tissues. Distance given is from the nucellar surface of the crease (cf. Fig. 1).

^{14}C Distribution Determined by Microdissection

The concentration of ^{14}C per unit volume in the crease tissues, as determined by counting of tissues dissected from serial sections, is shown in Figure 6. Sample heterogeneity limits the extent of useful quantitative interpretation in some regions. This is especially true of the "xylem" and "phloem," which simply indicates sections where these tissues were prominent compared to other sections; these samples consisted mostly of vascular parenchyma (Fig. 1). The same tissues were also sometimes poorly infiltrated in some regions, resulting in fragmentation and partial loss of sections. Finally, in the transition between cell types, one or two successive samples contained both cell types.

In general appearance, the ^{14}C distributions shown in Figure 6 reinforce those obtained from the microautoradiographs, with the important distinction that counting of dry-sectioned tissues eliminated complications arising from partial leaching of label from the sections by water. Also, the counting statistics are far more precise than for the relatively small number of grains counted in the autoradiographs.

Perhaps the most interesting region of ^{14}C distribution lies between the surface of the nucellar projection and the xylem. Here, fortunately, the tissue samples were also "purest," except at transitions between the tissues. At all sampling times, there was a shallow gradient from the nucellar surface through the nucellus and chalaza, with ^{14}C-specific activity increasing somewhat more than 2-fold over a distance of about 200 μm. Immediately past the chalazal boundary, there was a sharp increase of 2- to 3-fold in ^{14}C concentration in the vascular parenchyma over a distance of about 80 μm.

Effect on Crease Sugar Pools of Removing Grains from the Ear

Fisher and Gifford (1987) demonstrated that the endosperm cavity sap sucrose pool declines rapidly after wheat grains are removed from the ear. Although the initial rate of decline was slower than that expected from the rate of sucrose utilization by the endosperm (i.e. the grain-filling rate), we speculated that this might be due to continued movement into the cavity of sucrose from pools in the crease tissues. This was confirmed by the observations shown in Figure 7, which document the response of sucrose and hexose pools in the crease tissues to removal of grains from the ear. Virtually the entire sucrose pool in the crease tissues appeared to be available for movement into the endosperm cavity.

In contrast to sucrose, the crease hexose pool did not decline in excised grains, indicating that it was not available for transport. This is consistent with the absence of labeling of the crease hexose pool during ^{14}C-assimilate movement into the grain (see above).

Compartmental Analysis

The simplest model for sucrose pools in the wheat grain consists of three compartments (crease tissues, endosperm

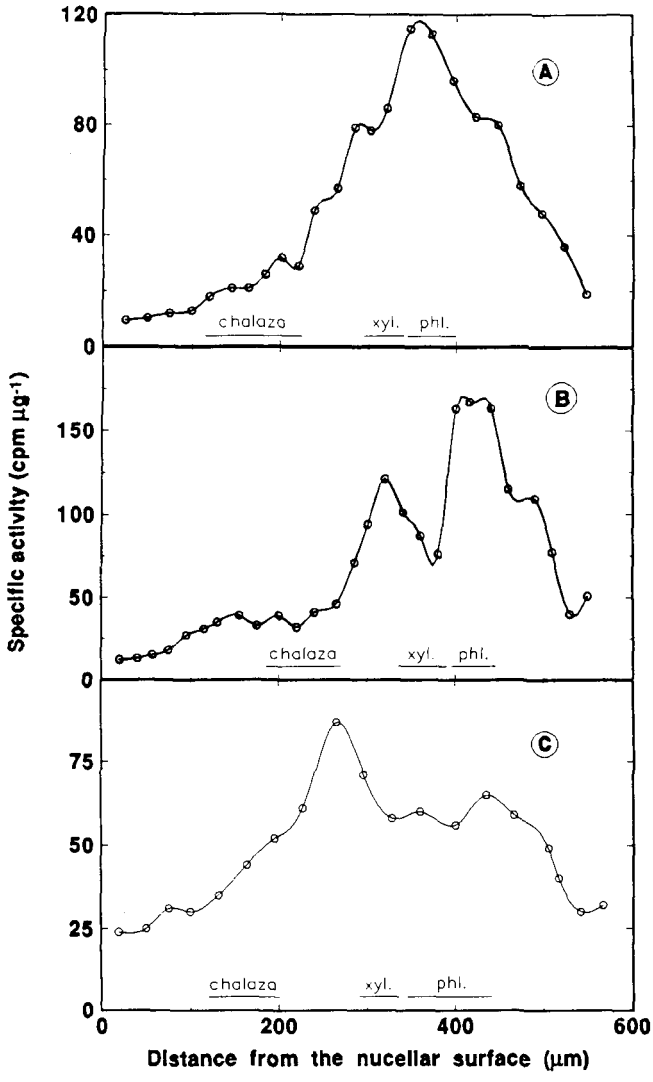

Figure 6. Specific activity of [^{14}C]sucrose on a volume (section weight) basis in epoxy-embedded crease tissues sampled at the times indicated in Figure 3. Distances given are from the nucellar surface of the crease tissues of the same specimens shown in Figure 4. xyl., Xylem; phl. phloem.

cavity, and endosperm) in series. However, because only unidirectional transport through the pools will be considered (with a minor exception), the endosperm pool will not be explicitly included. Pool sizes for the crease and endosperm cavity were based on the means of many tissue assays for various purposes. It should be noted that the endosperm cavity pool size varies considerably more than the crease pool, because both the cavity volume and sap concentration vary substantially (about 0.5–6 µL for the former, 40–120 mM for the latter). In the context of phloem unloading and post-phloem transport, the most important sucrose pool is that in the crease tissues. The size of this pool is much less variable, at 299 ± 70 nmol (n = 108). The rate of sucrose movement through the pools, given the grain-filling rate under these conditions of 1.94 ± 0.12 mg^{-1} of grain d^{-1} (Fisher, 1990), was taken to be 220 nmol h^{-1}. This assumes that sucrose makes up 75% of the dry weight entering the grain and that 20% of it is lost by respiration (Evans and Rawson, 1970; Fisher, 1990).

With an important correction, the input kinetics for the model were taken as the specific activity of sucrose in the peduncle sieve tubes (Fig. 2; upper dotted curves in Fig. 8). The required correction arises from the fact that, in the light, a substantial portion of the carbon for grain growth is supplied by photosynthesis within the ear, a contribution that will dilute the specific activity of [^{14}C]sucrose arriving from the peduncle. Thus, in the dark, when all of the carbon required for the ear must be imported, the mass transport rate through the peduncle is about 105 µg h^{-1} grain^{-1} under our growth conditions, whereas in the light it is only about 61 µg h^{-1} grain^{-1} (Fisher, 1990). If we assume that nongrain ear structures have a respiratory demand of about 10 µg h^{-1} grain^{-1} (Evans and Rawson, 1970), the incoming sucrose-specific activity is assumed to be diluted by a factor of 0.64 (61 µg h^{-1} grain^{-1}/95 µg h^{-1} grain^{-1}). These input kinetics are indicated as the lower dotted line in Figure 8.

On first consideration, it would appear that the specific activity of phloem exudate from the grain pedicels should be more representative of that entering the grain. Its specific activity did, in fact, appear to be somewhat lower than that from the peduncle (Fig. 2). However, the pedicel exudation rate was quite rapid compared with normal translocation rates. On average, 85 ± 30 nmol of sucrose were collected in 1 to 2 min, >10 times the rate of sucrose movement into the grain. Only a very small fraction of this could have been supplied by the few adjacent glumes. Most would have had to come from the main conducting pathway of the rachis and peduncle and would be diluted only slightly by unlabeled carbon from the glumes.

When the assumed input kinetics are used, a simple two-compartment model, in series with unidirectional transport through the compartments, comes quite close to accounting for the observed ^{14}C kinetics (Fig. 8A) in the crease tissues and endosperm cavity. The model could not be modified appreciably without predicting results that conflicted unacceptably with experimental data. A minor modification, suggested by the autoradiographs, is to assume that some of the sucrose (e.g. that in peripheral cells of the crease tissues) is not in a transport pool itself but exchanges with sucrose more

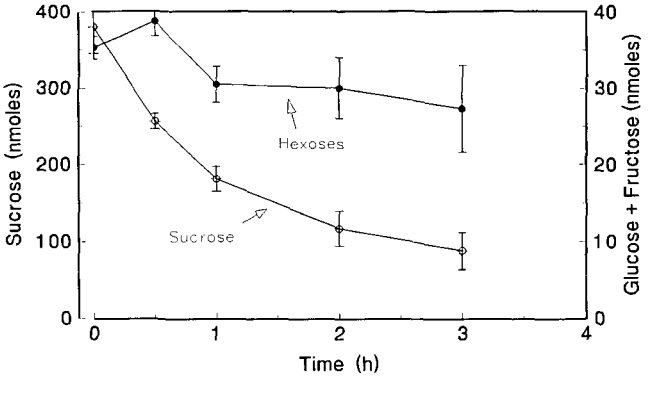

Figure 7. Response of crease sucrose and hexose pools to the removal of grains from the plant.

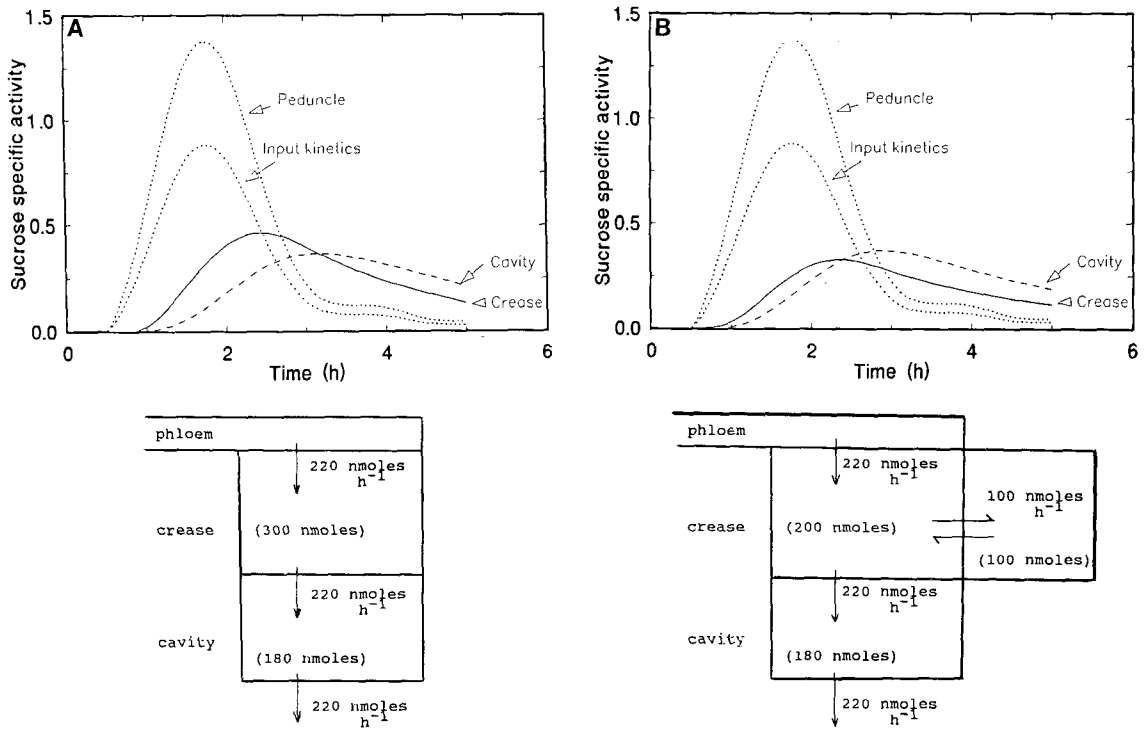

Figure 8. Compartmental models of [^{14}C]sucrose kinetics in the wheat grain. The models, with the constants used, are shown below the graphs. The kinetics of [^{14}C]sucrose-specific activity are those shown in Figure 2. The same kinetics, multiplied by a factor of 0.64 to account for dilution of imported ^{14}C by photosynthesis in the ear, were used as input kinetics for the models.

directly in the line of movement from the phloem to the chalaza. In Figure 8B, one-third of the crease sucrose has been placed in a pool in exchange with the transport pool, with a turnover time of 1 h. This results in a more rapid increase of cavity specific activity, which then increases above that of the crease at longer times. This appears to be inconsistent with our observations. However, our perfusion data suggest that there may be an appreciable "back-flux" of sucrose from the endosperm into the endosperm cavity (N. Wang and D.B. Fisher, unpublished observations). Basically, this would have the effect of reducing cavity-specific activity below that shown in Figure 8B, making its predicted kinetics more similar to experimental values.

DISCUSSION

Assimilate pools in the maternal tissues of a seed play a central role in post-phloem transport to embryonic tissues. In wheat grains, where assimilates must pass through the crease tissues to reach the endosperm (Ugalde and Jenner, 1990), we have shown that the sucrose in these tissues consists basically of a single well-mixed compartment. As shown by others (Sakri and Shannon, 1975; Ho and Gifford, 1984), sucrose moves without inversion from the phloem to the endosperm. This knowledge is fundamental for confident interpretation of observations concerning sucrose movement into the grain, especially where experimental conditions alter the transport rate. Because the pool is maintained by phloem unloading and is depleted by release of sucrose from the nucellus, a change in the pool size provides a useful indication of which of these component transport steps is affected by an experimental treatment. Significantly, the size of the pool is maintained within a relatively small range, suggesting that some particular steady-state concentration may be an important factor in reaching a balance between the rates of phloem unloading and solute release to the apoplast.

The microautoradiographs support the interpretation that the crease sucrose pool is well mixed. More important, in combination with measurements of specific activity on a volume basis, they suggest the presence of transport-related gradients within the crease tissues. That is, given the conclusion that sucrose-specific activity is fairly uniform at any one time within the crease, gradients in activity per unit volume must largely reflect sucrose concentration gradients, at least in those cells in which sucrose is turning over rapidly. This interpretation is less applicable where transport is not occurring or is very slow, as in the pericarp. It is also subject to ambiguity in the nucellus, at least within the surface cell layers, because the specific activity of sucrose there would be expected to match more closely that of the endosperm cavity.

The living nucellar cells bordering the chalaza are almost certainly the site of solute release into the apoplast. Apoplastic tracers move readily through nucellar walls but show very limited movement in chalazal walls (N. Wang and D.B. Fisher, unpublished observations), which are encrusted with sudanophilic materials (Zee and O'Brien, 1970; Cochrane, 1983). Also, owing to their wall invaginations, nucellar cells

have been categorized as "transfer cells" (Cochrane, 1983). Unfortunately, the substantial loss of ^{14}C from nucellar cells in the autoradiographs creates uncertainty concerning extracellular versus cellular concentrations there.

Given the above reservations, only approximate calculations of probable sucrose gradients are appropriate, but they are, nevertheless, instructive. From the nucellar surface through the nucellus and chalaza, the sucrose concentration appears to increase by about 2-fold along a smooth gradient. The latter observation is notable, because this path covers a transition from dead to living cells about halfway through the nucellus and the transition from nucellus to chalaza. Despite these transitions, the data suggest a pathway of uniform transport properties. Although the concentration of endosperm cavity sucrose was not measured here, 60 mM is a representative value, suggesting a sucrose concentration gradient of approximately 3×10^{-3} mol cm^{-3} cm^{-1} (6×10^{-2} mol L^{-1}/200 μm). Given the diffusion coefficient of sucrose (5.2×10^{-6} cm^2 s^{-1}) and ignoring barriers to diffusion, this gradient would sustain a sucrose flux density of 1.5×10^{-8} mol cm^{-2} s^{-1}. The actual flux density, given an import rate of 220 nmol h^{-1} over an area of 10^{-2} cm^2 (length × width of the chalaza), is 0.6×10^{-8} mol cm^{-2} s^{-1}. The two figures are remarkably similar, suggesting either an unusually low resistance to diffusive movement for both the transmembrane and cell-to-cell pathways and/or a contribution to movement by bulk flow.

The data in Figure 6 also suggest a gradient in sucrose concentration in the vascular parenchyma cells bordering the chalaza. Continuing the estimate of 120 mM sucrose in the chalaza, this suggests concentrations of about 250 to 350 mM in the vascular parenchyma near the phloem, where the concentration is about 600 mM (Fisher and Gifford, 1986; Fisher, 1990). This estimate of sucrose concentration in the vascular parenchyma cells is marginally acceptable, given the mean concentration of crease sucrose of 195 ± 16 mM (n = 16). The apparent concentration gradient bordering the chalaza is quite sharp. Although it presumably reflects the occurrence of rapid sucrose movement through these cells, the reasons for such a steep gradient here are not immediately evident.

Received May 27, 1992; accepted October 7, 1992.

LITERATURE CITED

Christy AL, Fisher DB (1978) Kinetics of ^{14}C-photosynthate translocation in morning glory vines. Plant Physiol **61:** 285–290

Cochrane MP (1983) Morphology of the crease region in relation to assimilate uptake and water loss during caryopsis development in barley and wheat. Aust J Plant Physiol **10:** 473–491

Donovan GR, Jenner CF, Lee JM, Martin P (1983) Longitudinal transport of sucrose and amino acids in the wheat grain. Aust J Plant Physiol **10:** 31–42

Ellis EC, Spanswick RM (1987) Sugar efflux from attached seed coats of *Glycine max* (L.) Merr. J Exp Bot **38:** 1470–1483

Evans LT, Rawson HM (1970) Photosynthesis and respiration by the flag leaf and components of the ear during grain development in wheat. Aust J Biol Sci **23:** 245–254

Fisher DB (1978) The estimation of sugar concentration in individual sieve-tube elements by negative staining. Planta **139:** 19–24

Fisher DB (1990) Measurement of phloem transport rates by an indicator-dilution technique. Plant Physiol **94:** 455–462

Fisher DB, Frame JM (1984) A guide to the use of the exuding-stylet technique in phloem physiology. Planta **161:** 385–393

Fisher DB, Gifford RM (1986) Accumulation and conversion of sugars by developing wheat grains. VI. Gradients along the transport pathway from the peduncle to the endosperm cavity during grain filling. Plant Physiol **82:** 1024–1030

Fisher DB, Gifford RM (1987) Accumulation and conversion of sugars by developing wheat grains. VII. Effect of changes in sieve tube and endosperm cavity sap concentrations on the grain filling rate. Plant Physiol **84:** 341–347

Fisher DB, Housley TL (1972) The retention of water-soluble compounds during freeze-substitution and microautoradiography. Plant Physiol **49:** 166–171

Fisher DB, Macnicol PK (1986) Amino acid composition along the transport pathway during grain filling in wheat. Plant Physiol **82:** 1019–1023

Gifford RM, Thorne JH (1986) Phloem unloading in soybean seed coats. Dynamics and stability of efflux into attached "empty ovules." Plant Physiol **80:** 464–469

Ho LC, Gifford RM (1984) Accumulation and conversion of sugars by developing wheat grains. V. The endosperm apoplast and apoplastic transport. J Exp Bot **150:** 58–73

Jenner CF (1974) Factors in the grain regulating the accumulation of starch. *In* RL Bieleski, AR Ferguson, MM Cresswell, eds, Mechanisms of Regulation of Plant Growth, Bulletin 12. The Royal Society of New Zealand, Wellington, New Zealand, pp 901–908

Jones MGK, Outlaw WH, Lowry OH (1977) Enzymic assay of 10^{-7} to 10^{-14} moles of sucrose in plant tissues. Plant Physiol **60:** 379–383

Lingle SE, Chevalier P (1984) Movement and metabolism of sucrose in developing barley kernels. Crop Sci **24:** 315–319

Minchin PEH, Thorpe MR (1989) Carbon partitioning to whole versus surgically modified ovules of pea: an application of the *in vivo* measurement of carbon flows over many hours using the short-lived isotope carbon-11. J Exp Bot **40:** 781–787

O'Parka KJ (1990) What is phloem unloading? Plant Physiol **94:** 393–396

Patrick JW, Offler CE, Wang HL, Wang X-D, Jin S-P, Zhang W-C, Ugalde TD, Jenner CF, Wang N, Fisher DB, Felker FC, Thomas PA, Crawford CG (1991) Assimilate transport in developing cereal grains. *In* JL Bonnemain, S Delrot, WJ Lucas, J Dainty, eds, Recent Advances in Phloem Transport and Assimilate Compartmentation. Ouest Editions, Nantes, France, pp 233–243

Redgwell RJ (1980) Fractionation of plant extracts using ion-exchange Sephadex. Anal Biochem **107:** 44–50

Sakri FA, Shannon JC (1975) Movement of ^{14}C-labeled sugars into kernels of wheat (*Triticum aestivum* L.). Plant Physiol **55:** 881–889

Sheppard CS (1962) Basic Principles of the Tracer Method. John Wiley & Sons, New York

Ugalde TD, Jenner CF (1990) Route of substrate movement into wheat endosperm. I. Carbohydrates. Aust J Plant Physiol **17:** 693–704

von Arx E, Neher R (1963) Eine multidimensionale Technik zur chromatographischen Identifizierun von Aminosauren. J Chromatogr **12:** 329–341

Zee SY, O'Brien TP (1970) Studies on the ontogeny of the pigment strand in the caryopsis of wheat. Aust J Biol Sci **23:** 1153–1171